Commentary on the temperature-dependent viscosity of supercooled liquids: a unified activation scenario

2009 J. Phys.: Condens. Matter 21 504104

(http://iopscience.iop.org/0953-8984/21/50/504104)

J. Phys.: Condens. Matter **21** (2009) 504104 (9pp) doi:10.1088/0953-8984/21/50/504104

Commentary on the temperature-dependent viscosity of supercooled liquids: a unified activation scenario

Akihiro Kushima[1], **Xi Lin**[2] **and Sidney Yip**[1,3]

[1] Department of Nuclear Science and Engineering, Massachusetts Institute of Technology, Cambridge, MA 02139, USA
[2] Department of Mechanical Engineering and Division of Materials Science and Engineering, Boston University, Boston, MA 02215, USA
[3] Department of Materials Science and Engineering, Massachusetts Institute of Technology, Cambridge, MA 02139, USA

Received 1 June 2009, in final form 15 September 2009
Published 23 November 2009
Online at stacks.iop.org/JPhysCM/21/504104

Abstract
Recent progress in describing the viscosity of vitrified liquids through an effective temperature-dependent activation barrier offers a new look at the basis for classifying fragile and strong glasses. By considering the activated state kinetics of model fragile and strong liquids, we identify a common structure in the temperature variation of their activation barriers. A unified description is proposed in which all glass formers can exhibit strong and fragile behavior in principle, and correspondingly two strong–fragile dynamic crossovers are indicated. Our deductions are based only on atomistic calculations using specific interatomic interactions. Thus the results are model predictions subject to further studies and experimental confirmation. On the other hand, the justification for the method being used to obtain the effective activation barriers is based on a direct experimental test of the calculated viscosities.

(Some figures in this article are in colour only in the electronic version)

1. Introduction

Viscous liquids by definition are characterized by slow structural relaxation. The shear viscosity $\eta(T)$ of a glass former typically increases by some 15 orders of magnitude from its normal liquid temperature to the glass transition temperature where the viscosity has a value of 10^{12} Pa s. Despite an abundance of measurements showing such behavior, no theory is yet able to explain the wide range of viscosity variations from fundamental considerations. Because viscosity is a measure of the product of shear modulus and a relaxation time τ, the challenge is to understand the drastic slowing down in temporal relaxation with undercooling.

In this paper, written on the occasion of the 60th birthday celebration of Francesco Mallamace who has made significant contributions to the understanding of structural arrest in liquids, we discuss the implications of two recent atomistic calculations of the viscosity of fragile [1] and strong [2] glass-forming liquids. In these studies a method was introduced to sample the transition state pathways in a vitrified liquid and perform a statistical analysis to extract an effective (coarse-grained) temperature-dependent activation barrier, $\bar{Q}(T)$. We begin by showing that the method, denoted as the single-path approximation (SPA), can provide an acceptable description of fragile (super-Arrhenius) behavior in the case of a binary Lennard-Jones (BLJ) model liquid [1], as well as a description of strong (Arrhenius) behavior in the case of a model of liquid silica [2]. The question then arises as to what else can be learnt by combining these two sets of results. We find from a comparison of $\bar{Q}(T)$, that both barriers have basically a common bi-level structure, namely a low activation energy at high temperatures, high activation energy at low temperatures, and fragile behavior in the intermediate temperature range. On the basis of this generic description one can rationalize all the essential features of the viscosity and activation barrier results in the BLJ and silica model studies. A prediction

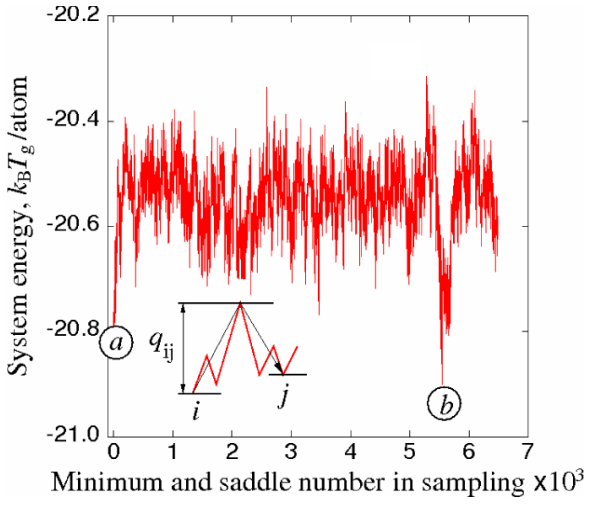

Figure 1. TSP trajectory of a supercooled binary Lennard-Jones (BLJ) system generated by the autonomous basin climbing sampling algorithm [1]. The high and low ends of the zigzag trace indicate the saddle point and local minima energies, respectively. Energy is expressed in T_g which is 0.37 in reduced units, a value obtained in the calculation of the shear viscosity (see figures 3 and C.1). See appendix B for an explanation of the inset and the significance of the two minima labeled *a* and *b*.

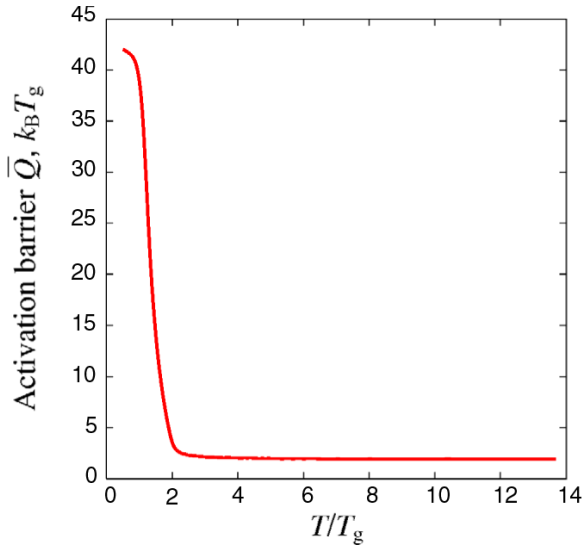

Figure 2. Effective temperature-dependent activation barrier $\bar{Q}(T)$ for a BLJ liquid obtained from the TSP trajectory shown in figure 1 by a statistical analysis (see appendix B for details).

of this scenario is the existence of two dynamic crossovers between the regimes of fragile and strong behavior, which is not compatible with classifying the glass-forming liquids simply as either fragile or strong.

2. Activation energy description of fragile temperature behavior

The effective activation barrier central to our discussions can be introduced in different ways. One is to appeal to transition state theory and write the shear viscosity of a liquid in the form [3]

$$\eta(T) = \eta_o \exp\left[\frac{\bar{Q}(T)}{k_B T}\right]. \quad (1)$$

Proposed as early as 1930 [4], equation (1) is widely used empirically to correlate experimental data. The prefactor η_o is to be determined by matching $\eta(T)$ to a known value at a certain temperature. While we will use equation (1) later to predict $\eta(T)$, we stress here that our intent is to obtain $\bar{Q}(T)$ through a systematic procedure that involves sampling the potential energy surface of the system. Consider the $3N$-dimensional potential energy function $\Phi(\underline{r}_N)$, where $\underline{r}_N$ denotes an atomic configuration of the N-particle system. We imagine that temporal relaxation of the supercooled liquid means the system is undergoing a sequence of atomic configuration changes whereby it samples a series of local energy minima. See appendix A for a description of an algorithm to activate a system to climb out of any potential well in order to traverse across a potential energy surface with multiple local minima and saddle points [1]. The system evolution is therefore represented by a trajectory in the form of a sequence of energy states alternating between local minima and saddles. A typical sequence, which we will call a transition state pathway (TSP) trajectory, obtained by using the BLJ model [5] is shown in figure 1. It should be noted that detailed information on the connectivity between the various energy minima and the saddle points that governs the temperature variation of the effective activation barrier $\bar{Q}(T)$ is contained in this trajectory. In figure 1 the glass transition temperature T_g, defined as $\eta(T_g) = 10^{12}$ Pa s, is used as an energy unit for the later purpose of comparing liquids which have different T_g.

From a TSP trajectory a corresponding coarse-grained (effective) temperature-dependent activation barrier can be extracted by a statistical analysis method, denoted as SPA and described in appendix B. This method allows us to predict the temperature variation of the viscosity using equation (1). The calculated effective activation barrier $\bar{Q}(T)$, shown in figure 2 for the BLJ model, has a remarkably simple two-level behavior [1]. The barrier is low and constant at high temperature, rises sharply in the interval $T/T_g \sim 1$–2 and appears to level off at a value about ten times greater than the high temperature level. It can be seen in appendix B that the barrier is made up of two contributions, a thermodynamic component that relates an average energy minimum to the temperature of supercooling (recall the concept of the inherent structure of liquids [6], shown in figure B.2) and a kinetic component correlating an effective activation energy with the depth of the local potential well (cf figure B.1). Each component has a shape similar to that of $\bar{Q}(T)$, although individually not as sharp as the combined result. Having extracted $\bar{Q}(T)$ we predict the viscosity using equation (1), in the process we take the high temperature limit where most liquid viscosities have a canonical value of 10^{-5} Pa s and thus fix η_o. With this procedure and combining figure 2 with equation (1) we have a prediction of $\eta(T)$ with no free parameter.

The resulting viscosity is shown in figure 3, along with experimental data for several fragile liquids [7]. In displaying the calculation and experimental data we express temperature

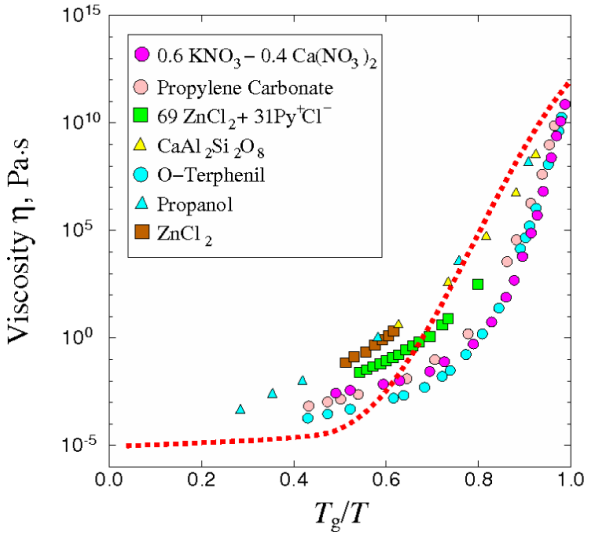

Figure 3. Temperature variation of viscosity calculated from equation (1) with $\bar{Q}(T)$ taken from figure 2 (dashed curve); symbols denote various measurements on fragile liquids [7].

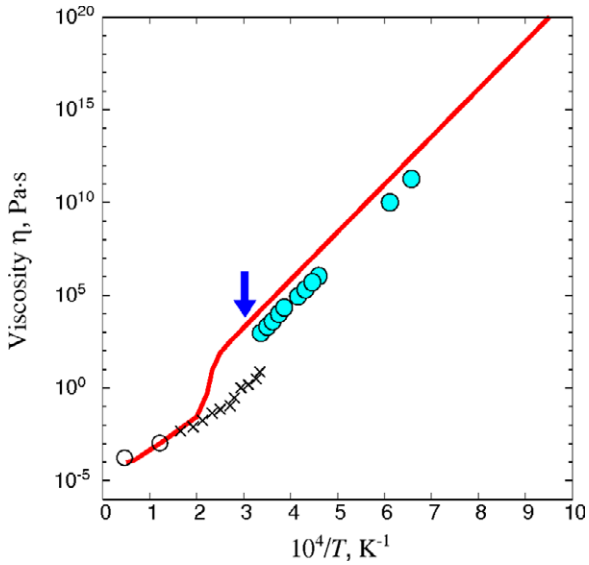

Figure 4. Temperature variation of viscosity of supercooled silica predicted by the SPA method and using equation (1) (solid curve) [2] along with experimental data (closed circles) [7]. Also shown are two sets of MD simulations (crosses [12] and open circles [13]). The arrow indicates a crossover between fragile and strong behavior suggested by simulations of entropy and diffusivity in a model silica [14].

in non-dimensional form, T/T_g. For the BLJ model T_g has been determined to be 0.37 in reduced units (see appendix C). We see that the combination of equation (1) and our calculated $\bar{Q}(T)$ describes qualitatively an overall 'fragile' behavior expressed by the set of experimental data. A significant aspect of figure 3 is the demonstration of a theoretical method capable of calculating the viscosity from room temperature to the glass transition temperature. Reflecting on the nature of the SPA method (appendix B) that leads to the resulting viscosity, we see it is essentially a mean-field description in which the system is assumed to follow a single activation path, one that is associated with the highest activation energy (see the path traced out in figure B.1). Thus SPA is expected to be an upper-bound estimate of $\bar{Q}(T)$ while ignoring the smearing effects of a distribution of possible activation paths. This understanding provides an explanation of the discrepancy in figure 3 between the SPA result and the experimental data, leaving aside the fact that none of the liquids measured are supposed to be well described by the BLJ model. To further justify our interpretation of the experimental test in figure 3, we consider an alternative and improved method of calculating $\eta(T)$ using the same TSP trajectory information. This is a method based on linear response theory in statistical mechanics which gives the viscosity directly, without invoking equation (1). In this method, which we call the network model, we adopt the Green–Kubo formalism [8] to derive the viscosity for a network model system of coupled nodes (see appendix C) [9]. The network model is theoretically more rigorous than the SPA; it is also more realistic because it considers explicitly all possible couplings between the multitude of local energy minima in the sampled trajectory [10]. The results of predicting $\eta(T)$ using the network model are shown in figure C.1. The agreement between the calculation and experiment is seen to improve considerably. On the basis of figures 3 and C.1 we conclude that the temperature behavior of vitrified fragile liquids can be qualitatively explained. To our knowledge, these are the first results of this kind.

3. Activation energy description of strong temperature behavior

The SPA method of TSP sampling and statistical analysis to obtain $\bar{Q}(T)$ has also been applied [2] to a model of liquid silica [11], well known to be a typical strong glass former [7]. The predicted $\eta(T)$, shown in figure 4, is seen to compare well with the experimental data. Given that one expects SPA results to be upper bounds, the modest overestimate in the absolute value of $\eta(T)$ is reassuring. For the relatively simple potential model adopted [11] T_g is predicted to be 1580 K [2], while the experimental value is 1446 K [7]. Thus our silica results, which are in explicit agreement with available experimental data, contribute to the validation of the SPA method. Above the temperature range of experimental data, the SPA results show a smooth transition from the portion that overlaps with the experimental data to a portion that overlaps with MD simulations [12, 13], in a manner that suggests two closely spaced dynamic crossovers. As the viscosity decreases with increasing temperature, the behavior undergoes a strong-to-fragile crossover, followed by a second crossover, this time from fragile back to strong. In the comparison with MD, we see agreement in the low-viscosity range where MD simulations can be expected to be reliable. In the high-viscosity end of the comparison the MD results do not indicate any fragile behavior; however, this is a difficult region for MD due to the slow relaxation of the stress correlation function. Any problem with convergence would result in an underestimate by MD. Using the same interatomic potential model, a study of entropy and diffusion properties using MD has been reported revealing a fragile–strong transition at 3300 K (indicated by the arrow in figure 4) [14]. Thus the possibility of a system,

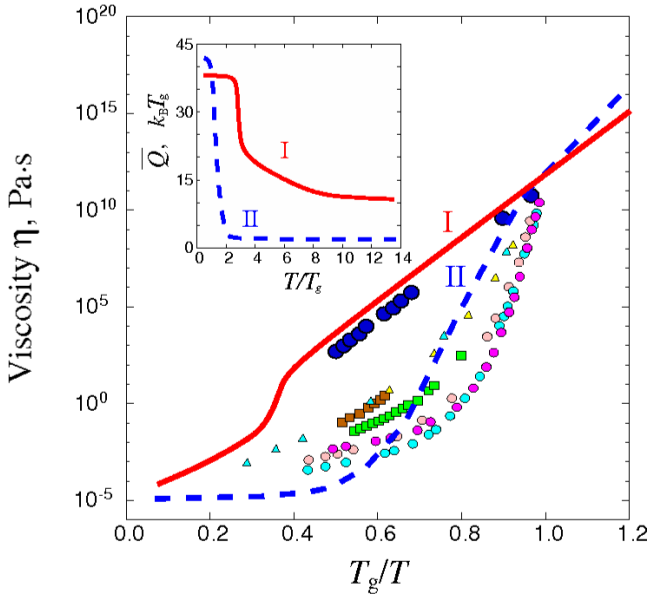

Figure 5. Comparison of viscosity calculations for silica (solid curve labeled I) and BLJ (dashed curve labeled II). Also shown are experimental data which appeared previously in figures 3 and 5. The inset shows the coarse-grained activation barriers for the two model systems labeled consistently with the viscosity results. For the silica model T_g is found to be 1580 K [2], while the experimental value is 1446 K [7].

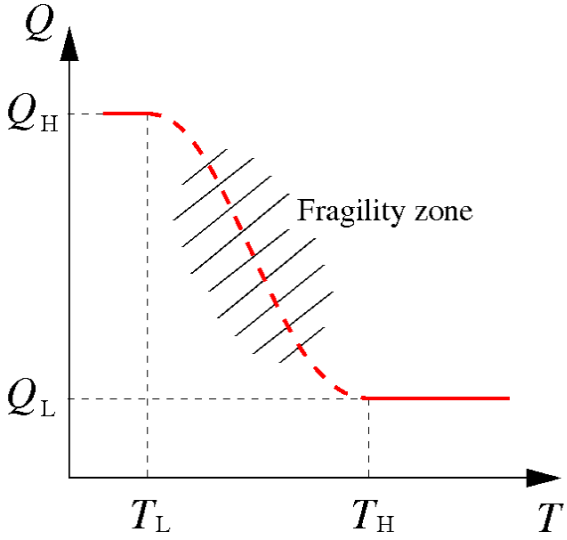

Figure 6. Schematic of a generic coarse-grained activation barrier with a bi-level structure. All symbols are defined in the text.

generally regarded as strong, showing a transition to fragile behavior is an interesting open question. Recently a fragile to strong transition in supercooled water has been demonstrated by a combination of neutron scattering, MD simulation and extended mode-coupling theory studies [15].

4. A generic activation model

Assuming the calculated temperature behavior shown in figures 3 and 4 are reasonable, we can compare the activation barriers to probe the nature of fragile and strong behavior ascribed to vitrified liquids normally classified as either fragile or strong. We display the BLJ and silica viscosity predictions together in figure 5 along with experimental data as reminders of the approximate nature of the theoretical curves. Additionally the corresponding effective activation barriers are shown in the inset of figure 5. Notice the difference in the temperature scales in the viscosity and activation barrier plots, one being the reciprocal of the other.

The BLJ system (dashed curve) is seen to exhibit fragile behavior in a temperature range different from the region where we have found liquid silica to be fragile. From our discussions of figures 2 and 3, fragile behavior is associated with an increase in the activation barrier with decreasing temperature. Indeed, in the inset in figure 5 two features are quite prominent. The activation barrier increase is considerably larger and the associated temperature range more sharply confined for the BLJ relative to that for silica. We also see the conventional way of displaying $\eta(T)$ brings out more fully the fragile behavior of the BLJ model (figure 3), but not the fragile behavior of oxide liquids (figure 4). In terms of their activation barriers $\bar{Q}(T)$ (figure 5 inset) the fragile behavior manifests in a complementary way, with the silica results more broadly displayed. These considerations suggest an idealization that captures the essence of temperature-dependent activation seen in both systems. What we mean is that both BLJ and silica results point to a bi-level form of $\bar{Q}(T)$, illustrated in figure 6.

In our conceptual description, a generic activation barrier $\bar{Q}(T)$ is simply a step with upper and lower levels separated at a certain height. We visualize it as a curve with roughly horizontal segments at two ends and an intermediate segment in the middle. The particular shape of $\bar{Q}(T)$ is characterized by two sets of parameters (Q_H, T_L) and (Q_L, T_H), which control the limiting behavior at low and high temperatures, respectively. In the transition region between T_L and T_H, the barrier is expected to follow a smooth interpolation between Q_H and Q_L with an inflection point. One can see the form shown in figure 6 captures well the results we have calculated for the BLJ and silica models. Also it can be rationalized by simple intuitive considerations of activated state kinetics. A system evolving at temperatures above T_H can expect to encounter a distribution of many shallow potential wells which, at the coarse-grained level, could be represented by a constant activation energy Q_L. At the opposite limit of temperatures below T_L, the system is very likely to be trapped in a localized, deep potential well and therefore requires a high activation energy Q_H to escape. This scenario is consistent with the inherent structure concept, see figures B.2 and 2.

In the particular case of BLJ and silica, we see their low-T segments are similar, Q_H, ~40–50 $k_B T_g$, whereas the high-T barriers are quite different, $Q_L \sim 2k_B T_g$ (BLJ) and 10 $k_B T_g$ (silica). Given that Q_H (Q_L) governs the slope $\frac{d\eta}{dT}$ at T_H (T_L), this contrast is also apparent in figure 5. The larger difference between Q_H and Q_L for BLJ shows up as a more extended and pronounced fragility range. The larger value of Q_L for silica compared to BLJ can be attributed to the nature of chemical bonding in these two models. This difference also manifests in the mechanisms of individual activation events which one

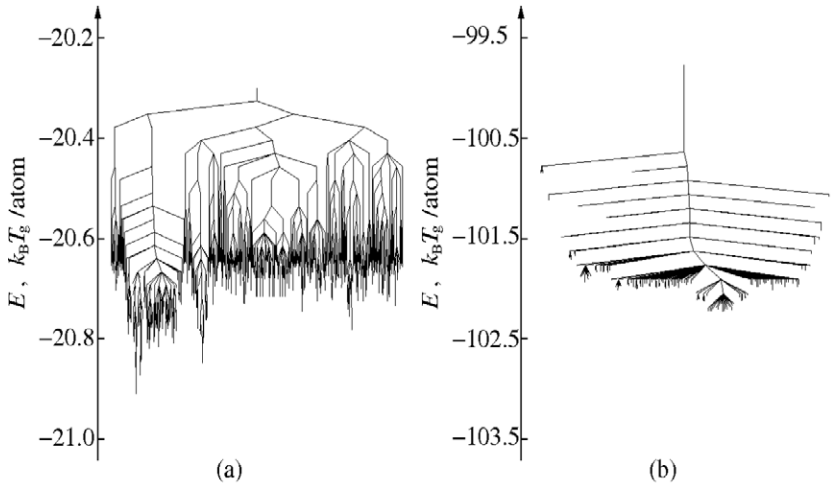

Figure 7. Disconnectivity graphs [16] of BLJ (a) and silica (b) constructed from their respective TSP trajectories.

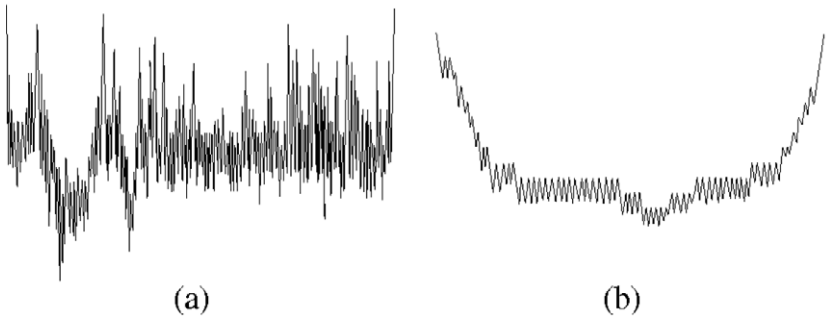

Figure 8. Potential energy landscape profiles for BLJ (a) and silica (b) deduced by taking a one-dimensional cut across the disconnectivity graphs shown in figure 7.

can probe through the atomic configurations associated with the TSP trajectory [1, 2]. Thus the generic barrier can be viewed as an interpolation between the two limiting values, and the transition range, between T_L and T_H, becomes the *fragility zone*. This is a way to bring out the common origin of strong and fragile behavior which may not be apparent from only a consideration of the viscosities (figure 5).

A direct consequence of figure 6 is the existence of two transitions between strong and fragile behavior, around T_H and T_L. We expect that in the vicinity of the melting point the behavior of $\eta(T)$ should be reasonably Arrhenius until the temperature decreases to T_H where a crossover to fragile behavior occurs. With further supercooling $\eta(T)$ is fragile until T_L, where a second dynamic crossover occurs from fragile to strong. Given our interpretation of Q_L above, we expect T_H should depend on chemical bonding, whereas T_L should be a collective characteristic that is system-insensitive other than scaling with T_g. We believe these two crossovers should be a universal feature of glass formers.

5. Potential energy landscape signatures of fragility

We have thus far emphasized the effective activation barrier $\bar{Q}(T)$ as a way to extract quantitative information from TSP trajectories. There are other forms of mapping and classifying the contours and connectivity details of a potential energy landscape. A particular graphical representation is shown in figure 7 for the two prototypical systems we are examining. The local minima and saddle point energies are visualized through a tree-like structure of vertical lines (states) and branch points (saddles), a mapping process known as a 'disconnectivity graph' [16, 17]. By reference to an energy axis, each vertical line starts at the local minimum and extends upward to connect to other potential wells and branches through various vertex points. Of interest here is the contrast of the multitude of splitting and large relative fluctuations in the depth of local minima, features that characterize the BLJ graph, with a relatively sparse structure seen in the silica graph. From a disconnectivity graph one can derive a one-dimensional profile (cut) of the $3N$-dimensional potential energy surface. The resultant potential energy profiles for BLJ and silica are shown in figure 8. We see that silica, known for its strong temperature behavior, may be described as a broad-base funnel with relatively small fluctuations in the depth of local minima, and an overall 'smooth' appearance [16, 17]. On the other hand, the BLJ profile shows the features of a rough energy landscape, conventionally associated with fragile behavior [18, 19].

6. Summary

The present discussion is intended to comment on the nature of fragile versus strong behavior in the viscosity of vitrified liquids. Our deliberations are motivated by a method to calculate an effective temperature-dependent activation barrier that could describe either fragile or strong behavior. The model systems studied display fragile as well as strong behavior, each over an appropriate temperature range, even though one system (BLJ) is generally regarded as fragile and the other (silica) as strong. This combination of results calls into question the practice of classifying glass-forming liquids as either fragile or strong. In the same spirit a unified picture of supercooled liquids and the universality of two dynamic crossovers is suggested. We think what is important is not whether the Q_{H} and Q_{L} segments should be strictly or approximately temperature-dependent, but that these two activation barriers can be significantly different. On this basis it may be appropriate to define *fragility as a dynamically necessary interpolation* between the barriers at low and high temperatures, which is the message conveyed by figure 6. Our deductions have evolved entirely within the framework of the energy landscape and inherent structure of liquids, with essentially no input from experimental observations. Thus an experimental test of the predicted fragile–strong crossovers would be very timely. Moreover, there are implications for the current perspectives on the glass transition phenomenon [19–21] that would be worth pursuing.

Acknowledgments

This work is based on studies supported by a grant from Corning Incorporated. We are grateful to our collaborators, Ju Li, Jacob Eapen, Xiaofeng Qian, John C Mauro and Phong Diep, for their contributions, and to S-H Chen for discussions.

Appendix A. The autonomous basin climbing algorithm (ABC)

We have implemented a procedure to lift a system of particles out of any potential well by a series of activation–relaxation steps. The algorithm [1] is a modification of the method known as metadynamics which was devised by Laio and Parrinello for escaping from free-energy minima [22]. Here we will describe the procedure only schematically. As shown in figure A.1, one can start with the system in a potential minimum E_1^{m}, step (a) in figure A.1. A prescribed energy penalty function is then imposed and the system is allowed to relax to settle into a new energy-minimized configuration. At the end of each activation–relaxation sequence, the system will find itself in a new energy state, typically higher than before the penalty imposition, step (b) in the figure. The process of activation–relaxation is repeated until the system finds itself in an appreciably lower energy state which indicates it has gone over a saddle point and settled into an adjacent local minimum, step (c). As the process continues, the previous local minima are not visited because the penalty functions providing the activation before are not removed; thus the system is encouraged to always sample new local minima, step (d). Repeating the sequence of starting from an initial local minimum E_1^{m} to cross a saddle point E_1^{s} to reach a nearby local minimum E_2^{m}, etc, thus generates a transition state pathway (TSP) trajectory. An example of three local minima and two saddle points is depicted in figure A.1. We have used this procedure to generate transition state pathway trajectories which are a sequence of local minima and saddle point energies, an example of which is shown in figure 1. For verification the algorithm has been tested against known solutions for the problem of adatom diffusion on the surface of Al(001) [1].

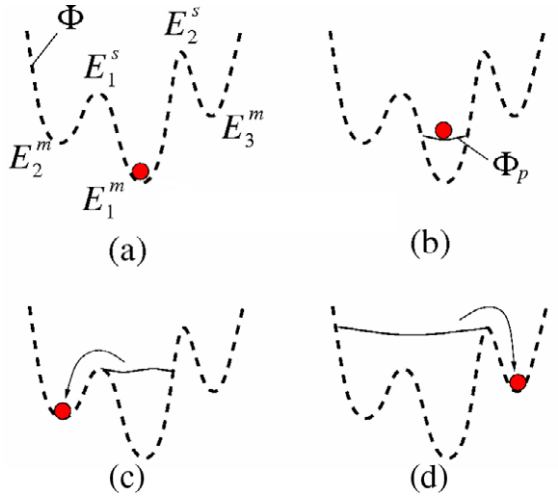

Figure A.1. Schematic illustration explaining the basin filling method. Dashed and solid lines indicate original potential energy surface and penalty potential, respectively. Penalty functions push the system out of a local minimum to a neighboring minimum by crossing the lowest saddle barrier [1].

Appendix B. Activation barrier analysis

We describe here the essential steps of the statistical analysis method used to determine the effective (coarse-grained) temperature-dependent activation barrier $\bar{Q}(T)$ from a TSP trajectory [1]. In the inset of figure 1 we define q_{ij} as the activation energy that connects the two local minima i and j. For each pair of local minima, no matter how far separated they are in the trajectory we have an activation energy. Suppose we do not care about the state label i and concentrate only on the two variables, the depth of the initial energy minimum, E_i, and the magnitude of q_{ij}, $Q = |q_{ij}|$. We imagine that we go through the entire trajectory to count the number of (i, j) combinations that lead to certain values of Q and E_i, and use the data to construct a density-of-states surface in the two variables Q and E_i. The result obtained from such an analysis of figure 1 is shown in figure B.1. We imagine the sampling of the system energy begins at a deep minimum labeled as a, and after sampling some 5×10^3 local minima of various depths it arrives at another deep minimum labeled as b. What is shown in figure 1 is just this alternating sequence of local minima and local maxima (saddle point) energies. Keep in

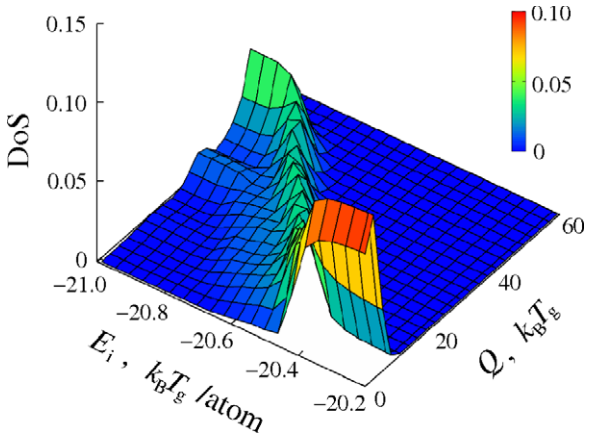

Figure B.1. Density-of-states surface in the plane of the two variables in the statistical analysis of the TSP trajectory (figure 1), the activation energy Q and the well depth of a local minimum. The 'ridge' on this surface traces out a correlation between Q and E_i, which provides one of two components in the make-up of the coarse-grained activation barrier shown in figure 2.

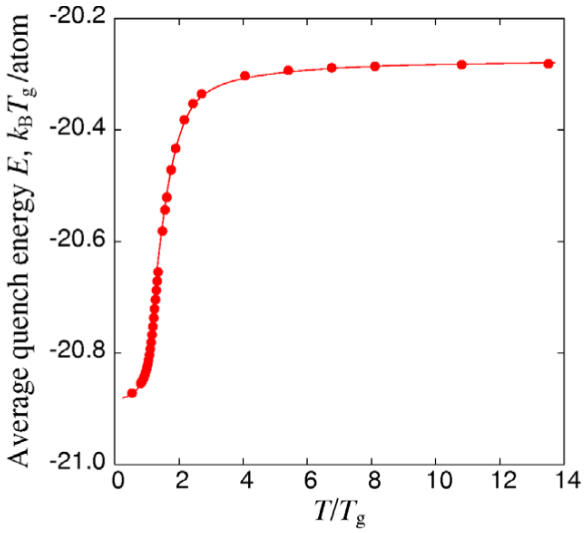

Figure B.2. Variation of average inherent structure with temperature of supercooling for a BLJ liquid [2]. Such a result was first presented in a discussion of energy landscape signatures [19]. Here T_g is 0.37 in reduced units (see appendix C).

mind this is only one transition state pathway (TSP) trajectory that connects minima a and b, there would be many others which also connect a with b. We want to emphasize here that, while a single trajectory, limited by the system size and extent of the sampling, may not seem sufficient, we have found that this much trajectory is already useful for obtaining an effective temperature-dependent activation barrier of the system. Part of the reason lies in the statistical analysis which we perform to extract the effective activation barrier, a process which amounts to coarse-graining over a distribution of activation barriers across the sampled trajectory.

In figure B.1 the surface is seen to be primarily a single ridge running diagonally across the Q–E_i plane. The highest (largest density of states) portion of this ridge lies in the corner region of shallow minimum and low Q. From here the ridge runs diagonally at a somewhat lower DOS level toward the corner region of deep minimum and high Q. Projecting this ridge onto the Q–E_i plane gives a Q versus E_i curve, showing an interesting variation of Q with E_i; low Q when E_i is shallow rising sharply to high Q when E_i becomes deep. The $Q(E_i)$ curve provides an estimate of how much activation energy Q is needed to climb out of an energy minimum of depth E_i. This is the kinetics part of the input to the effective temperature-dependent activation barrier. The thermodynamics part enters when we relate the energy minimum E_i to the temperature T. For this we consider the study of inherent structure of liquids by quenching from molecular dynamics simulations at various temperatures [6, 1]. The variation of the averaged quenched energy with temperature is shown in figure B.2. This energy is insensitive to T at high T, but decreases quite strongly when T is below about twice T_g. Now, as a coarse-graining procedure we assume we can replace E_i, the depth of the local energy minimum sampled in the TSP trajectory, in the Q versus E_i relation by the average inherent structure which is correlated with temperature T in the manner shown in figure B.2. Thus we arrive a cross plot of Q as a function of T which is shown in figure 2. The cross plot thus transforms an effective activation energy $Q(E_i)$, extracted from a TSP trajectory analysis, into another coarse-grained activation barrier $\bar{Q}(T)$ which is temperature-dependent. While the process may be seen as a mapping between E_i and T through the average inherent structure, we are not able to provide a systematic justification. It is therefore a physically motivated approximation which is perhaps best rationalized by its consequence as we will see below.

We should note that the process of obtaining $\bar{Q}(T)$ naturally combines two contributions to this effective activation barrier. The temperature variation of $\bar{Q}(T)$ is sharper than either the increase of Q with decreasing E_i or the decrease of average inherent structure $\bar{E}(T)$ with lowering T. The former represents the effects of activated state kinetics, while the latter may be regarded as a thermodynamic effect contributing to the sharp increase of $\bar{Q}(T)$ in the characteristic temperature range. We will call our formulation of $\bar{Q}(T)$ the single-path approximation (for reducing the activation energy surface to a projection along a diagonal path). Since the path is chosen to follow 'the ridge' in the density-of-states distribution, we expect this approximation to be an upper-bound estimate. We have tested the reliability of the activation barrier obtained by SPA in the case of BLJ by comparing with results derived from viscosity data on fragile liquids (cf figure 16 in [1]). In addition, SPA results for model silica are compared with experiments in figure 4.

Appendix C. The network model for viscosity

We consider a system of N interacting particles with volume Ω at temperature T. The system is characterized by an ensemble of states (nodes in the Markov network), index by $\{i\}$, each is

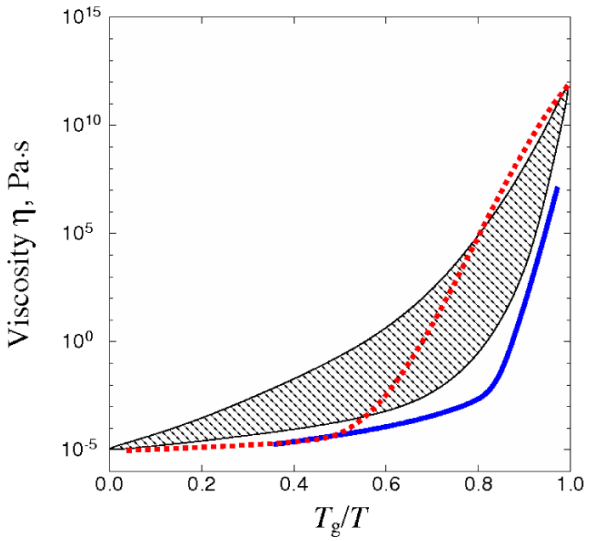

Figure C.1. Temperature variation of viscosity calculated by the network model with TSP trajectory input from figure 1 (solid curve) [10]. A more heuristic result given by the SPA formulation, given in figure 3, is shown for comparison (dashed curve). Also shown are the experimental data given in figure 3, as a shaded band.

associated with a free energy

$$F_i = -k_B T \ell n \int \mathrm{d}x^{3N} \exp\left(-\frac{V(x^{3N})}{k_B T}\right) + \text{const} \qquad \text{(C.1)}$$

and a shear stress

$$\sigma_i = \frac{1}{\Omega}\left\langle N k_B T \prod + \sum_{n=1}^{N} x_n \otimes \partial_{x_n} V \right\rangle_i . \qquad \text{(C.2)}$$

In (C.1) and (C.2) V is the interatomic interaction potential. We assume the states are connected by a set of transition rates

$$a_{ij} = \nu_o \exp(-q_{ij}/k_B T) \qquad \text{(C.3)}$$

where ν_o is a constant prefactor, a frequency that depends on the application context, and q_{ij} is the activation barrier separating state j from state i. The Markov network model is thus specified by the nodal energies, stress and the activation barriers $\{F_i, \sigma_i, q_{ij}\}$. To use this model to calculate the shear viscosity $\eta(T)$ of a liquid we recall the Green–Kubo formalism in linear response theory where $\eta(T)$ is given by the expression

$$\eta(T) = \frac{\Omega}{k_B T}\int_0^\infty \mathrm{d}\tau \langle \sigma(t)\sigma(t+\tau)\rangle \qquad \text{(C.4)}$$

where $\langle \sigma(t)\sigma(t+\tau)\rangle$ is the time-dependent shear stress correlation function. Since we assume that at any given time the system has to reside at one of the states, we can write the shear stress as

$$\sigma(t) = \sum_i \sigma_i p_i(t) \qquad \text{(C.5)}$$

with $p_i(t)$ being an indication function, equal to unity if the system is at state i at time t, otherwise it is zero. To further exploit the assumption of the system being in one of the states at any given time, we introduce a time-dependent nodal stress:

$$\begin{aligned} g_i(\tau) &= \langle \sigma(t+\tau)\rangle_{p_i(t)=1} \\ &= \sum_j \sigma_j \langle p_j(t+\tau)\rangle_{p_i(t)=1} \end{aligned} \qquad \text{(C.6)}$$

such that the stress correlation function becomes an average over nodes

$$\langle \sigma(t)\sigma(t+\tau)\rangle = \sum P_i \sigma_i g_i(\tau) \qquad \text{(C.7)}$$

with

$$P_i = \exp\left(-\frac{F_i}{k_B T}\right) \qquad \text{(C.8)}$$

being the probability that the system is in state i. Thus the viscosity also becomes a nodal average

$$\eta(T) = \frac{\Omega}{k_B T}\sum_i P_i \sigma_i G_i \qquad \text{(C.9)}$$

with

$$G_i(T) = \int_0^\infty \mathrm{d}\tau\, g_i(\tau). \qquad \text{(C.10)}$$

The stress $g_i(\tau)$ has the physical interpretation of an average stress at time τ given that the system was in state i at an earlier time t. It can be shown that $g_i(\tau)$ satisfies a balance equation which can be solved exactly [9, 10]. As a result

$$\eta(T) = \frac{\Omega}{k_B T}\sum_i P_i \sigma_i \frac{1}{a_i}(A(\omega = 0^+)^{-1}\tilde{\sigma})_i \qquad \text{(C.11)}$$

where

$$(A(\omega))_{ij} = \delta_{ij} - \frac{a_{ij}}{\omega + a_j}, \qquad a_i = \sum_j a_{ij}. \qquad \text{(C.12)}$$

Thus from the TSP trajectory given in figure 1 we can identify each local energy minimum E_i as F_i, and use each activation energy q_{ij} to define the transition rate a_{ij}, which leaves the prefactor ν_o as the only constant to be determined in a calculation of $\eta(T)$.

The results of the network model are compared in figure C.1 with the SPA estimate, as well as the experimental data shown in figure 3, now represented by a band [1]. The improved agreement seen is quite consistent with our theoretical expectations. The fact that the network model indeed accounts for a more pronounced 'fragile' behavior similar to the band of experimental data supports our previous assertion that discrepancy between the SPA and experiment should be attributed to the neglect of coupling effects in activated state kinetics. In the network model study we estimated T_g though the definition $\eta(T_g) = 10^{12}$ Pa s, obtaining $T_g = 0.37$ in reduced units for the BLJ potential. For this potential model the mode-coupling theory temperature T_c has been determined to be 0.435 [5]. The ratio of $T_c/T_g \sim 1.3$, being consistent with expectations [7], serves as another check of the general reliability of our results. Furthermore, we have modified our SPA approach by including an entropy correction in the manner of Adam–Gibbs [23], and found the results similar to the network model calculation seen in figure C.1. We interpret this to mean that entropic effects and corrections for coupling effects work in the same direction in that they both represent additional complexities in the system energy landscape.

References

[1] Kushima A, Lin X, Li J, Eapen J, Qian X, Mauro J C, Diep P and Yip S 2009 *J. Chem. Phys.* **130** 224504
[2] Kushima A, Lin X, Li J, Eapen J, Qian X, Mauro J C, Diep P and Yip S 2009 *J. Chem. Phys.* at press
[3] Brush S G 1962 *Chem. Rev.* **63** 513
[4] Andrade E N da C 1930 *Nature* **125** 309
[5] Kob W and Andersen H C 1995 *Phys. Rev.* E **51** 4626
[6] Stillinger F H and Weber T A 1982 *Phys. Rev.* A **25** 978
[7] Angell C A 1988 *J. Phys. Chem. Solids* **49** 863
[8] McQuarrie D A 1973 *Statistical Mechanics* (New York: Harper and Row) p 512
[9] Li J http://mt.seas.upenn.edu/Stuff/vis/Notes/main.pdf
[10] Li J, Kushima A, Lin X, Eapen J, Qian X, Mauro J C, Diep P and Yip S 2009 *J. Chem. Phys.* submitted
[11] Feuston B P and Garofalini S H 1988 *J. Chem. Phys.* **89** 5818
[12] Horbach J and Kob W 1999 *Phys. Rev.* B **60** 3169
[13] Eapen J and Kushima A 2009 *J. Chem. Phys.* submitted
[14] Saika-Voivod I, Poole P H and Sciortino F 2001 *Nature* **412** 514
[15] Chen S H, Zhang Y, Lagi M, Chong S H, Baglioni P and Mallamace F 2009 Evidence of dynamic crossover phenomena in water and other glass-forming liquids: experiments, MD simulations and theory *J. Phys.: Condens. Matter* **21** 504102
[16] Becker O and Karplus M 1997 *J. Chem. Phys.* **106** 1495
[17] Wales D J 2006 *Int. Rev. Phys. Chem.* **25** 237
[18] Stillinger F H 1988 *J. Chem. Phys.* **88** 7818
[19] Sastry S, Debenedetti P G and Stillinger F H 1998 *Nature* **393** 554
[20] Dyre J C 2006 *Rev. Mod. Phys.* **78** 963
[21] Trachenko K and Brazhkin V V 2008 *J. Phys.: Condens. Matter* **20** 075103
[22] Laio A and Parrinello M 2002 *Proc. Natl Acad. Sci.* **99** 12562
[23] Adam G and Gibbs J H 1965 *J. Chem. Phys.* **43** 139